Title:
Isogeometric Shape Optimization of Reissner-Mindlin Shell Structures for Maximizing Fundamental Eigenfrequency

Authors:
Xiaoxiao Du, duxiaoxiao@buaa.edu.cn, Beihang University
Zhihao Zhang, zhangzhih@buaa.edu.cn, Beihang University
Zhaoyun Liu, kkrylzy@buaa.edu.cn, Beihang University
Jiayi Li, caulijiayi@163.com, Beihang University
Wei Wang, jrrt@buaa.edu.cn, Beihang University
Gang Zhao, zhaog@buaa.edu.cn, Beihang University

Keywords:
Isogeometric Shape Optimization, Reissner-Mindlin Shell, Maximum Fundamental Eigenfrequency, Analytical Sensitivity

DOI: 10.14733/cadconfP.2025.172-177

Introduction:
The fundamental eigenfrequency is a critical parameter that must be considered in the design of engineering structures. A lower fundamental eigenfrequency increases the susceptibility of a structure to large vibrations under low-frequency excitations, due to resonance phenomena. Therefore, maximizing the fundamental eigenfrequency is essential to mitigate excessive vibrations during the structural design process. The primary factors influencing the fundamental eigenfrequency include the geometric shape and size, material properties, and boundary conditions of the structure. In recent years, structural optimization has increasingly focused on factors such as size, shape, topology, and material to achieve a maximized fundamental eigenfrequency [7, 8, 10].

Isogeometric analysis offers an integrated workflow for computer-aided design (CAD) and finite element analysis (FEA) by directly utilizing spline-based CAD models for numerical simulations, thereby eliminating the need for traditional mesh generation. This seamless design-through-analysis process significantly facilitates structural shape optimization. In this study, we extend the multi-patch isogeometric structural shape optimization framework introduced in [1] to optimize the fundamental eigenfrequency of shell structures. Structural analysis is performed using the Reissner-Mindlin shell theory. A gradient-based optimization algorithm, combined with analytical sensitivity analysis, is employed to solve eigenfrequency optimization problems. A numerical example is presented to demonstrate the effectiveness of the proposed method.

Free Vibration Analysis of Reissner-Mindlin Shell:
A multi-patch isogeometric Reissner-Mindlin shell method is employed for the numerical simulation of shell structures. The deformation behavior of shell structures is assumed to occur within the regime of small displacements and small rotations. A shell structure can be represented by its middle surface as

follows:

$$\boldsymbol{x}(\xi,\eta,\zeta)=\tilde{\boldsymbol{x}}(\xi,\eta)+\frac{t}{2}\zeta\boldsymbol{n}(\xi,\eta), \tag{2.1}$$

in which $\tilde{\boldsymbol{x}}(\xi,\eta)$ denotes the middle surface represented by NURBS patches; t is the thickness of the shell; $\boldsymbol{n}(\xi,\eta)$ indicates the unit normal vector; $\zeta\in[-1,1]$ is the parameter along the thickness direction.

The displacement of the shell structure is then written as

$$\boldsymbol{u}(\xi,\eta,\zeta)=\tilde{\boldsymbol{u}}(\xi,\eta)+\frac{t}{2}\zeta\left[\tilde{\boldsymbol{\theta}}(\xi,\eta)\times\boldsymbol{n}(\xi,\eta)\right], \tag{2.2}$$

where $\tilde{\boldsymbol{u}}(\xi,\eta)$ and $\tilde{\boldsymbol{\theta}}(\xi,\eta)$ denote the displacements and rotations of the middle surface. Using NURBS basis functions to interpolate the nodal displacements and rotations defined at control points, Eq. (2.2) can be rewritten as

$$\boldsymbol{u}(\xi,\eta,\zeta)=\sum_{i=0}^{n_{cp}}R_i(\xi,\eta)\left\{\tilde{\boldsymbol{u}}_i+\frac{t}{2}\zeta\left[\tilde{\boldsymbol{\theta}}_i\times\boldsymbol{n}(\xi,\eta)\right]\right\}, \tag{2.3}$$

in which $\tilde{\boldsymbol{u}}_i=[u_i,v_i,w_i]^T$ and $\tilde{\boldsymbol{\theta}}_i=[\theta_{xi},\theta_{yi},\theta_{zi}]^T$ represent the three displacements and three rotations defined at the i-th control point [4].

Arranging the translational displacements $\tilde{\boldsymbol{u}}_i$ and rotational displacements $\tilde{\boldsymbol{\theta}}_i$ into a 6×1 vector as $\bar{\boldsymbol{u}}_i$, the strain vector $\boldsymbol{\epsilon}$ in Voigt form can be given by

$$\boldsymbol{\epsilon}=[\epsilon_{xx},\epsilon_{yy},\epsilon_{zz},2\epsilon_{xy},2\epsilon_{yz},2\epsilon_{xz}]^T=\sum_{i=0}^{n_{cp}}\boldsymbol{B}_i\bar{\boldsymbol{u}}_i=\boldsymbol{B}\,\boldsymbol{u}, \tag{2.4}$$

where $\boldsymbol{B}$ denotes the strain-displacement matrix.

The solution for the free vibration analysis of shell structures, can be obtained by solving the following stiffness equation

$$(\boldsymbol{K}+\lambda_n\boldsymbol{M})\boldsymbol{u}_n=\boldsymbol{0}. \tag{2.5}$$

where $\boldsymbol{K}$ and $\boldsymbol{M}$ denote the stiffness matrix and the mass matrix, respectively; λ_n is the n-th frequency parameter and $\boldsymbol{u}_n$ is the eigenvector corresponding to λ_n. The eigenvector $\boldsymbol{u}_n$ is normalized using the mass matrix with $\boldsymbol{u}_n^T\boldsymbol{M}\boldsymbol{u}_n=1$. Assuming that the shell structure is constructed by n_{pth} NURBS patches, $\boldsymbol{K}$ and $\boldsymbol{M}$ can be computed as

$$\boldsymbol{K}=\sum_{I=1}^{n_{pth}}\int_{\Omega_I}\left(\boldsymbol{B}^T\boldsymbol{D}\boldsymbol{B}\right)d\Omega_I,\quad \boldsymbol{M}=\sum_{I=1}^{n_{ph}}\int_{\Omega_I}\left(\rho\boldsymbol{N}^T\boldsymbol{N}\right)\,d\Omega_I. \tag{2.6}$$

in which $\boldsymbol{D}$ represents the global constitutive matrix; $\boldsymbol{N}$ is the shape function matrix; Ω_I indicates the physical space of I-th NURBS patch. For a detailed derivation of the isogeometric Reissner-Mindlin shell formulations, the reader is referred to [3, 4].

Isogeometric Shape Optimization:

The fundamental eigenfrequency, λ_1, can be maximized by minimizing the objective function $f=1/\lambda_1$. However, this objective function is discontinuous and may not be differentiable, which can adversely affect the convergence of the optimization process. Furthermore, optimizing a single eigenfrequency may lead to mode switching issues. To address these challenges, a multi-eigenfrequency objective function, as proposed in [5], is adopted:

$$f(\boldsymbol{h})=\left\{\sum_{i=1}^{n_\lambda}\left(\frac{1}{\lambda_i(\boldsymbol{h})}\right)^{\alpha}\right\}^{1/\alpha}, \tag{2.7}$$

where $\boldsymbol{h}$ denotes the set of design variables. Let $\boldsymbol{h} = (h_1, h_2, \cdots, h_{n_d})$, the shape optimization of a shell structure can be expressed as:

$$\begin{aligned} find \quad & \boldsymbol{h} \in \mathbb{R}^3 \\ min \quad & f = f(\boldsymbol{h}) \\ s.t. \quad & [\boldsymbol{K}(\boldsymbol{h}) + \lambda_n \boldsymbol{M}(\boldsymbol{h})]\, \boldsymbol{u}_n = \boldsymbol{0}, \\ & g(\boldsymbol{h}) = S(\boldsymbol{h})/S_0 - \gamma \leq 0, \\ & h_i^{min} \leq h_i \leq h_i^{max},\ i = 1, \cdots, n_d \end{aligned} \tag{2.8}$$

in which $S(\boldsymbol{h})$ is the area of the middle surface of the shell structure for a design set $\boldsymbol{h}$; S_0 denotes the initial area; γ is the prescribed area fraction; h_i^{min} and h_i^{max} denote the minimum and maximum limits of the i-th design variable h_i.

Within the framework of isogeometric shape optimization, a multi-level representation of the geometric model can be employed, with a coarse model used for design purposes and a denser model for analysis. The design variables are associated with the control points of the coarse design model. Let $\boldsymbol{P}$ and $\boldsymbol{Q}$ denote the control point vectors of the design model and the analysis model, respectively. A refinement or transformation matrix $\boldsymbol{R}$ is constructed based on the knot insertion and degree elevation algorithms of the NURBS technique, such that $\boldsymbol{Q} = \boldsymbol{R}\boldsymbol{P}$. Utilizing the adjoint method, the sensitivity of the k-th eigenvalue λ_k with respect to the dense control points $\boldsymbol{Q}$ can be computed by:

$$\frac{d\lambda_k}{d\boldsymbol{Q}} = \boldsymbol{u}_k^T \left(\frac{\partial \boldsymbol{K}}{\partial \boldsymbol{Q}} - \lambda_k \frac{\partial \boldsymbol{M}}{\partial \boldsymbol{Q}} \right) \boldsymbol{u}_k. \tag{2.9}$$

The expression for $\partial \boldsymbol{K}/\partial \boldsymbol{Q}$ is derived in detail in [1] and is not repeated here, while the term $\partial \boldsymbol{M}/\partial \boldsymbol{Q}$ can be derived as

$$\frac{\partial \boldsymbol{M}}{\partial \boldsymbol{Q}} = \rho \int_{\bar{\Omega}} \left\{ \frac{\partial \boldsymbol{N}^T}{\partial \boldsymbol{Q}} \boldsymbol{N} |\boldsymbol{J}| + \boldsymbol{N}^T \frac{\partial \boldsymbol{N}}{\partial \boldsymbol{Q}} |\boldsymbol{J}| + \boldsymbol{N}^T \boldsymbol{N} \frac{\partial |\boldsymbol{J}|}{\partial \boldsymbol{Q}} \right\} d\bar{\Omega}, \tag{2.10}$$

where $|\boldsymbol{J}|$ is the determinant of the Jacobian matrix and $\bar{\Omega}$ denotes the parametric space corresponding to the physical space Ω. The differentiation of the coarse control points $\boldsymbol{P}$ with respect to the design variable h_i is specified. Considering the refinement matrix and the differentiating chain rule, the sensitivity of the multi-eigenfrequency objective function, as given in Eq. (2.7), takes the form:

$$\frac{df}{dh_i} = \frac{\partial f}{\partial h_i} + \frac{\partial f}{\partial \lambda_k} \frac{\partial \lambda_k}{\partial \boldsymbol{Q}} \boldsymbol{R} \frac{\partial \boldsymbol{P}}{\partial h_i}. \tag{2.11}$$

At this stage, the sensitivity can be explicitly derived. The open-source framework, NLIGA [2], is utilized for numerical implementation, in conjunction with the open-source library NLOPT [6, 9] for solving the optimization problem.

Numerical Examples:

In this section, the shape optimization of a cylindrical shell is investigated. The geometric parameters, as illustrated in Fig. 1(a), are defined with $L = 60$m and $R = 10$m. The material properties are specified as: Young's modulus $E = 30$MPa, Poisson ratio $\nu = 0.3$, density $\rho = 2500$ Kg/m^3. The thickness of the shell takes $t = 0.5$m. The left end boundary is clamped.

The design model is represented by 16 quadratic elements, as depicted in Fig. 1(b). Along the length direction of the cylindrical shell, which aligns with the x-axis, there are six layers of control points. Each layer comprises nine control points. The design variable is assigned to the i-th layer of control points.

Consequently, the derivative of the j-th layer control point $\mathbf{P}_k^j$, as illustrated in Fig. 1(c), with respect to the design variable h_i, can be explicitly expressed as:

$$\begin{aligned}
&\frac{\partial \boldsymbol{P}_1^j}{\partial h_i} = \frac{\partial \boldsymbol{P}_9^j}{\partial h_i} = [0,1,0], \quad \frac{\partial \boldsymbol{P}_2^j}{\partial h_i} = \left[0, \frac{\sqrt{2}}{2}, \frac{\sqrt{2}}{2}\right], \quad \frac{\partial \boldsymbol{P}_3^j}{\partial h_i} = [0,0,1], \quad \frac{\partial \boldsymbol{P}_4^j}{\partial h_i} = \left[0, -\frac{\sqrt{2}}{2}, \frac{\sqrt{2}}{2}\right], \\
&\frac{\partial \boldsymbol{P}_5^j}{\partial h_i} = [0,-1,0], \quad \frac{\partial \boldsymbol{P}_6^j}{\partial h_i} = \left[0, -\frac{\sqrt{2}}{2}, -\frac{\sqrt{2}}{2}\right], \quad \frac{\partial \boldsymbol{P}_7^j}{\partial h_i} = [0,0,-1], \quad \frac{\partial \boldsymbol{P}_8^j}{\partial h_i} = \left[0, \frac{\sqrt{2}}{2}, -\frac{\sqrt{2}}{2}\right].
\end{aligned} \tag{2.12}$$

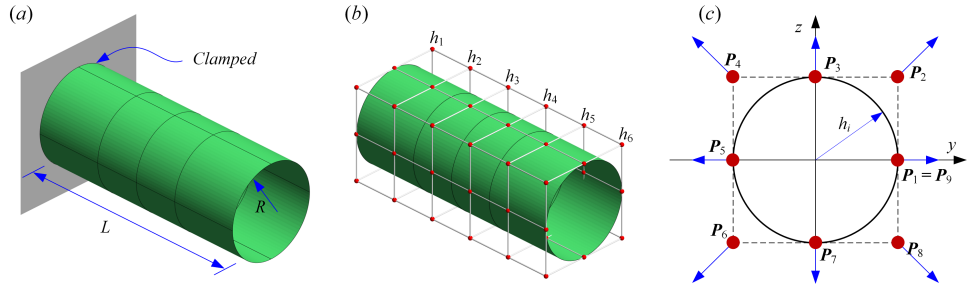

Fig. 1: Geometrical modeling of a cylindrical shell. (a)Geometrical dimensions; (b) Design model; (c) circumferential parametrization using the design variable.

We first examine the convergence of the eigenfrequencies for the initial cylindrical shell without shape optimization. The cylindrical shell is progressively refined into 4×4, 8×8, 12×12, 16×16, 24×24, 32×32, and 48×48 bi-quadratic elements. As illustrated in Fig. 2, it is observed that the first three eigenfrequencies converge to relatively stable values upon refinement to 24×24 elements. Conservatively, the refinement of 32×32 elements is adopted as the dense analysis model for subsequent shape optimization.

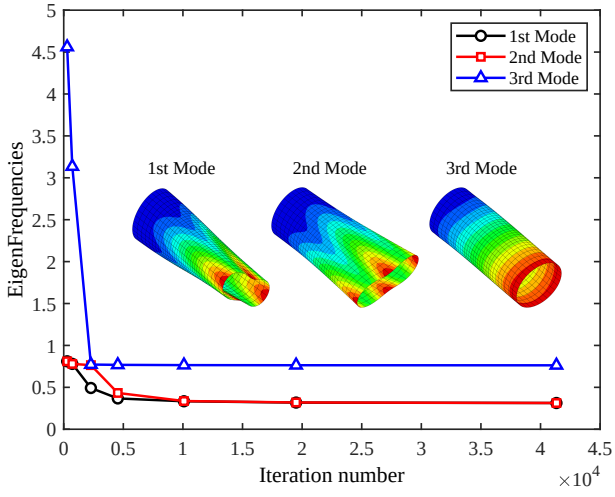

Fig. 2: Convergence of the first three eigenfrequencies and corresponding mode shapes of the initial cylindrical shell, without shape optimization.

The design variables are constrained to the range $[-5, 5]$, and the area is restricted to be smaller than the initial area throughout the shape optimization process. Figure 3 illustrates the history of the

shape optimization process, depicting both the objective function and the first-order eigenfrequency of the cylindrical shell. Convergence is achieved for both metrics after fifteen iterations. Notably, the radius of the left-end circle increases from 5m to 10m, while the radius of the right-end circle decreases from 10m to 5.6475m. Figure 4 presents the first twelve mode shapes of the optimized cylindrical shell. For quantitative comparison, Table 1 lists the first eight eigenfrequencies of the initial and optimized models, revealing a significant increase following shape optimization; in particular, the first-order eigenfrequency rises by 568.50%, from 0.3115 to 2.0827.

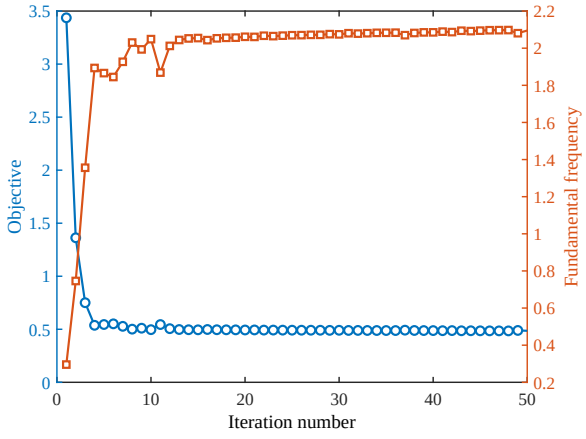

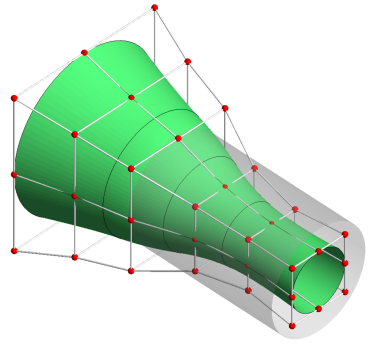

Design variable	h_1	h_2	h_3	h_4	h_5	h_6
Value at 50th step	5.0000	2.0617	0.0302	-3.6695	-5.0000	-4.3525

Fig. 3: Left: Optimization history of the objective function and the first-order eigenfrequency. Right: Optimized cylindrical shell at the 50th iteration, along with the corresponding design variables.

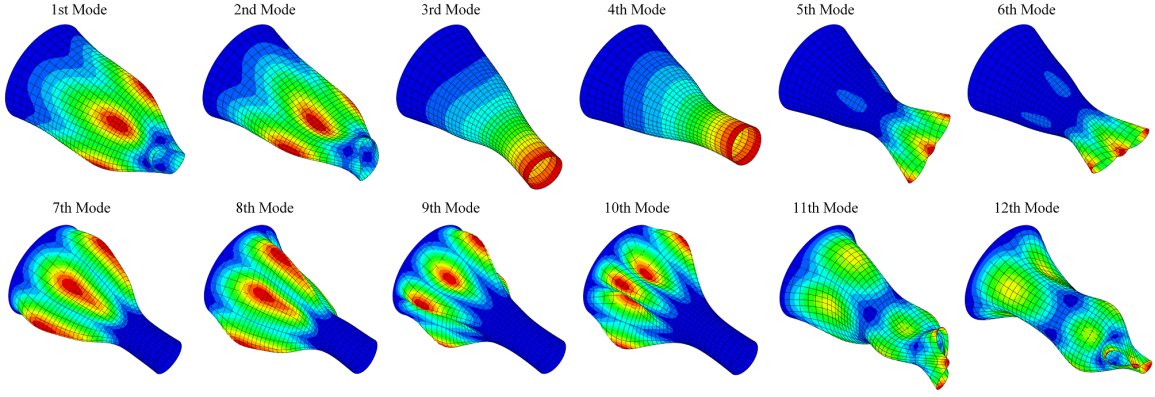

Fig. 4: The first twelve mode shapes of the optimized cylindrical shell.

Conclusions:

This study aims to maximize the fundamental eigenfrequency of shell structures using the isogeometric shape optimization method. A multi-level geometric representation strategy is implemented to effectively accommodate the distinct requirements of the design and analysis models. Analytical sensitivity formulations are derived to facilitate shape optimization. The numerical example demonstrates a successful increase in the fundamental eigenfrequency, validating the effectiveness of the proposed method.

Table 1: The first eight eigenfrequencies of the cylindrical shell, both before and after shape optimization.

Mode Sequence	1	2	3	4	5	6	7	8
Initial Model	0.3115	0.3115	0.7624	0.7624	1.6208	1.6208	2.6821	2.6821
Optimized Model	2.0827	2.0827	2.0937	2.0937	3.8159	3.8159	4.7250	4.7250
Increase (%)	568.60	568.60	174.62	174.62	135.43	135.43	76.168	76.168

Acknowledgement:

This research is partially supported by National Key Research and Development Program of China (Project No. 2023YFB3309000), Beijing Natural Science Foundation of China (Project No. 4242025), National Natural Science Foundation of China (Project Nos. 52175213 and 62102012) and Young Elite Scientists Sponsorship Program by CAST (Project No. 2022QNRC001).

Xiaoxiao Du, https://orcid.org/0000-0002-2324-1005

References:

[1] Du, X.; Li, J.; Wang, W.; Zhao, G.; Liu, Y.; Zhang, P.: Isogeometric shape optimization of reissner–mindlin shell with analytical sensitivity and application to cellular sandwich structures. Computer-Aided Design, 173, 103728, 2024. http://doi.org/10.1016/j.cad.2024.103728.

[2] Du, X.; Zhao, G.; Wang, W.; Guo, M.; Zhang, R.; Yang, J.: NLIGA: A MATLAB framework for nonlinear isogeometric analysis. Computer Aided Geometric Design, 80, 101869, 2020. http://doi.org/10.1016/j.cagd.2020.101869.

[3] Du, X.; Zhao, G.; Wang, W.; Liu, Y.; Zhang, P.; Han, P.; Cheng, H.: Parametric modeling and simulation of a simplified horizontal tail under the framework of isogeometric analysis. Computer-Aided Design & Applications, 21, 635–645, 2024. http://doi.org/10.14733/cadaps.2024.635-645.

[4] Du, X.; Zhao, G.; Zhang, R.; Wang, W.; Yang, J.: Numerical implementation for isogeometric analysis of thin-walled structures based on a Bézier extraction framework: nligaStruct. Thin-Walled Structures, 180, 109844, 2022. http://doi.org/10.1016/j.tws.2022.109844.

[5] Hirschler, T.; Bouclier, R.; Duval, A.; Elguedj, T.; Morlier, J.: A new lighting on analytical discrete sensitivities in the context of isogeometric shape optimization. Archives of Computational Methods in Engineering, 28(4), 2371–2408, 2021. http://doi.org/10.1007/s11831-020-09458-6.

[6] Johnson, S.G.: The NLopt nonlinear-optimization package. https://github.com/stevengj/nlopt, 2007.

[7] Nagy, A.P.; Abdalla, M.M.; Gürdal, Z.: Isogeometric design of elastic arches for maximum fundamental frequency. Structural and Multidisciplinary Optimization, 43, 135–149, 2011. http://doi.org/10.1007/s00158-010-0549-z.

[8] Shi, J.X.; Nagano, T.; Shimoda, M.: Fundamental frequency maximization of orthotropic shells using a free-form optimization method. Composite Structures, 170, 135–145, 2017. http://doi.org/10.1016/j.compstruct.2017.03.007.

[9] Svanberg, K.: A class of globally convergent optimization methods based on conservative convex separable approximations. SIAM Journal on Optimization, 12(2), 555–573, 2002. http://doi.org/10.1137/S1052623499362822.

[10] Xu, M.; Wang, S.; Xie, X.: Level set-based isogeometric topology optimization for maximizing fundamental eigenfrequency. Frontiers of Mechanical Engineering, 14, 222–234, 2019. http://doi.org/10.1007/s11465-019-0534-1.